Analysis of Bacterial Swimming Speed Approaching a Solid–Liquid Interface

Paul D. Frymier and Roseanne M. Ford
Dept. of Chemical Engineering, University of Virginia, Charlottesville, VA 22903

Previous experimental studies have found that surface interactions significantly affect the transport of motile bacteria through small tubes, along solid surfaces, and through porous media. However, the role that hydrodynamic forces play in the interactions between solid surfaces and motile bacteria remains unclear. In this study, the swimming speeds of populations of Escherichia coli bacteria were measured near (<10 μm) and far (>10 μm) from a flat glass surface at four ranges of orientations to the surface (0°–45°, 45°–90°, 90°–135°, and 135°–180°). Populations of bacteria close to the surface and moving in the orientation range most perpendicular (0–45°) to the surface experienced the greatest change in the swimming speed when compared to the population in the same orientation range located far from the surface. The decrease in swimming speed experienced by this population was on the same order as that predicted by hydrodynamic models of bacterial swimming near surfaces.

Introduction

Accurate prediction of the effect of surface interactions on the transport properties (such as the swimming speed) of bacteria is critical in the modeling of bacterial transport and *in situ* bioremediation rates in porous media, bacterial attachment to chemical process unit surfaces, and biofilm formation in bioreactors for product synthesis and industrial wastewater treatment. In a saturated porous medium (a contaminated groundwater aquifer, for example), the close proximity of surfaces affects the swimming speed of bacteria through hydrodynamic interactions between cells and solid surfaces and between the cells themselves. In addition, numerical simulations of biofilm formation indicate that when "slow-" and "fast"-swimming bacteria are present in a population adjacent to a solid surface, the biofilm formed will be populated preferentially by cells of the fast-swimming population. How much can we expect changes in cell swimming speed to effect these processes? In the case of bacterial transport, for example, the "random motility coefficient" (analogous to the diffusion coefficient for solute diffusion) is proportional to the square of the cell swimming speed (Lovely and Dalquist, 1975), so a 20% decrease in the swimming speed leads to a 36% decrease in the motility coefficient. For simulated biofilm formation, the authors of a recent study found that for two populations of bacteria (a "fast" population and a "slow" population whose swimming speed was half that of the fast population), the resulting simulated biofilm was composed of as much as twice as many of the fast-swimming cells (Eliashberg and Keasling, 1996). Clearly changes in the swimming speed significantly affect the distribution of swimming bacteria in a contaminated aquifer and in a biofilm. It is therefore important to be able to quantify the changes in swimming speed that bacteria can be expected to experience when encountering solid surfaces.

To study the mechanisms of bacteria–surface interactions, it is necessary to understand the physics of bacterial motion. Motile bacteria such as *Escherichia coli* are able to move about in a fluid through the rotation of 8–10 flagella located around the periphery of the cell body. By changing the direction of rotation of the flagella, an individual bacterium exhibits two distinct phases of motion, running and tumbling. In the running phase, a bacterium moves in an approximately straight path at speeds on the order of 20 μm/s for periods of approximately 1 s. In the tumbling phase, a bacterium exhibits little translational motion, but spins in place for a period of approximately 1/10 s, resulting in a random reorientation. A bacterium's motion through a homogeneous fluid medium as it alternates between running and tumbling is a random walk analogous to the Brownian motion of small

Additional address for P. D. Frymier: Dept. of Chemical Engineering, University of Tennessee, Knoxville, TN 37996.

particles. For a comprehensive review of the characteristic motion of mobile bacteria, see Berg (1993).

The hydrodynamics of motile bacteria swimming in a fluid medium are dominated by viscous and pressure forces and are governed by Stokes' equation (Brennen and Winet, 1977; Lighthill, 1976). Many of the experimental and theoretical studies of flagellar hydrodynamics have dealt with the development and verification of mathematical models for the motion of bacteria through homogeneous fluid media. Experimental studies have focused primarily on the speed at which the individual flagella rotate (Berg and Turner, 1979; Lowe et al., 1987; Manson et al., 1980), the speed at which bacteria move through a fluid (Berg and Brown, 1972; Myerscough and Swan, 1989; Ramia and Swan, 1994), the formation and motive force of the flagellar bundle (Manson et al., 1980; Schneider and Doetsch, 1974; Winet and Keller, 1976), and the effect of fluid viscosity on flagellar and body rotation (Berg and Turner, 1979; Lowe et al., 1987; Schneider and Doetsch, 1974). Theoretical studies that attempt to model the cell body and associated flagellar bundle can be roughly divided into two types: (1) those that utilize geometric and mathematical approximations of the flagellar bundle and cell body to derive simplified mathematical models (Chwang et al., 1972; Higdon, 1979a,b; Myerscough and Swan, 1989; Winet and Keller, 1976), and (2) those that allow for general cell body and flagellar bundle configurations (Phan-Thien et al., 1987; Ramia and Swan, 1994) and require numerical solution of the resulting set of partial differential equations. We note as an aside that all models of a complete bacterium currently known to us treat the flagellar bundle as a solid unit and do not model the flagellar bundle as a collection of individually rotating flagella. This assumption is likely to increase in validity with the viscosity of the fluid; studies have shown that flagellar propulsion is more efficient in viscous environments (Berg and Anderson, 1973; Schneider and Doetsch, 1974), and some researchers have suggested that this is because more flagella are able to join the bundle as the viscosity of the medium increases (Stocker, 1956).

Previous experimental studies of bacterial motion have confirmed the importance of accounting for bacteria–surface interactions when accurate measurements of the microscopic characteristics of bacterial swimming behavior are desired (Baba et al., 1991; Myerscough and Swan, 1989). Other researchers have shown the effect of surface interactions on macroscopic bacterial transport rates (Berg and Turner, 1990), while still others have shown that hydrodynamic effects between individual cells can influence the swimming speed of microorganisms when restricted to movement in small capillaries (Lui and Papadopoulos, 1995).

There have been several attempts to model the interactions between bacteria and surfaces. As was the case for models of bacterial motion in the absence of solid surfaces, models of bacteria–surface interactions are of essentially two types: (1) those that utilize approximations of the flagellar bundle to derive simplified mathematical models (Katz and Blake, 1975; Reynolds, 1965), and (2) those that allow solutions for general cell-body and flagellar-bundle geometries (Ramia et al., 1993). The model of Ramia et al. (of the second type described previously) predicts that a bacterium moving toward a solid surface will exhibit a decrease in swimming speed as it approaches the surface. This result agrees with predictions of the change in speed of inert colloid particles moving toward a solid surface (Brenner, 1961).

In this study, we used a tracking microscope to follow 90 individual bacteria moving in the presence of a solid surface. We showed that the speed of bacteria moving toward a solid surface decreases as the cell approaches the surface and that the measured change in speed was on the order of that predicted by two models derived from hydrodynamic forces: one specifically designed to model the flagellar propulsion of microorganisms near surfaces and the other based on the solution by Brenner (1961) of Stokes' equation for a sphere moving toward a solid surface through a viscous fluid. The data suggest that the appropriate model for flagellar propulsion lies somewhere between the two models, but further studies are necessary to discriminate between the two models.

Background

Fundamental work relevant to the study of the motion of bacteria has been done by researchers interested in the interactions between spherical particles and solid surfaces at low Reynolds number. For a slow-moving spherical particle in a viscous fluid, the force of drag resisting the motion of the sphere can be calculated from the solution to Stokes' equation for creeping flow around a sphere, which is given by Eq. 1a (Brenner, 1961):

$$F = \begin{cases} 6\pi\mu b U_\infty, & (h/b) = \infty, \quad \text{(a)} \\ 6\pi\mu b U \lambda(h/b), & (h/b) < \infty, \quad \text{(b)} \end{cases} \tag{1}$$

where μ is the fluid viscosity, h is the distance to a surface (taken as ∞ for an unbounded fluid), and U and b are the speed and radius of the sphere, respectively. If the shape of a bacterium can be approximated by a sphere and if it is swimming at a constant speed, the force provided by the flagella is equal to the resistance from the fluid and can be calculated by Eq. 1a.

Now, consider the case of a sphere moving toward a solid surface with speed U and whose center is a distance h from the solid surface (see Figure 1). The force on a sphere moving at a constant velocity U toward the solid wall will no longer remain constant, but will increase as the separation distance increases. Brenner (1961) gives the solution to the creeping flow equation for the force resisting the motion of the sphere as it approaches the solid surface perpendicularly, which was given as Eq. 1b, where λ is given by

$$\lambda = \frac{4}{3}\sinh\alpha \sum_{n=1}^{\infty} \frac{n(n+1)}{(2n-1)(2n+3)} \times \left[\frac{2\sinh(2n+1)\alpha + (2n+1)\sinh 2\alpha}{4\sinh^2(n+1/2)\alpha - (2n+1)^2\sinh^2\alpha} - 1 \right] \tag{2}$$

and

$$\alpha = \cosh^{-1}\left(\frac{h}{b}\right) = \ln\left\{\frac{h}{b} + \sqrt{\left[\left(\frac{h}{b}\right)^2 - 1\right]}\right\}. \tag{3}$$

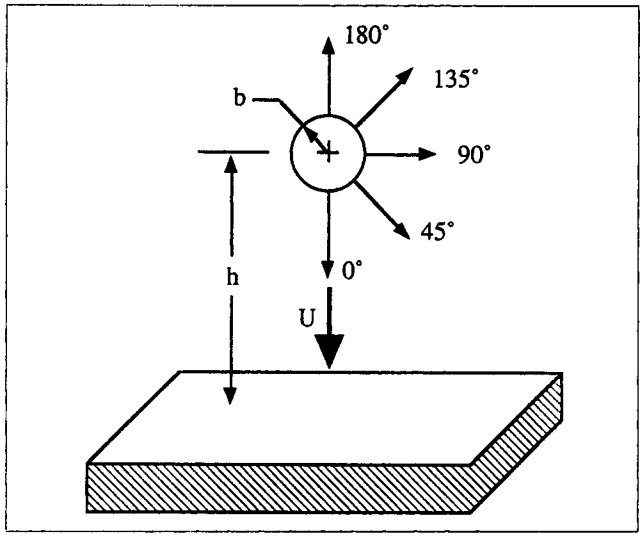

Figure 1. Definitions of angles and dimensions.

Equation 1a assumes the spherical particle of radius b is at a distance $h = \infty$ from the solid surface and is moving at a constant speed U_∞. Equation 1b assumes that the spherical particle is moving toward and perpendicular to (an orientation of 0° as defined here) the solid surface at a constant speed U at a distance $h \leq \infty$ from the surface.

By comparing Eqs. 1a and 1b, it can be seen that λ represents the increase in the force resisting the motion of the sphere due to the presence of the solid surface. If the sphere approaches the wall such that the force resisting its motion remains equal to its value in an unbounded fluid (at a separation distance of ∞), then its speed can be calculated by equating Eqs. 1a and 1b:

$$F_{h/b=\infty} = 6\pi\mu b U_\infty = 6\pi\mu b U\lambda = F_{h/b<\infty} \tag{4}$$

or

$$\frac{U}{U_\infty} = \lambda^{-1}. \tag{5}$$

The conditions under which this expression would be expected to yield a reasonable approximation of the speed of bacterium as it approaches a solid surface are (1) an approximately spherical cell body; (2) a flagellar bundle that produces a constant force; and (3) small inertial forces relative to viscous forces. For Reynolds numbers relevant to the motion of bacteria through water ($O(10^{-5})$), the third condition is valid (Brenner, 1961). The question of whether or not the flagellar bundle is capable of producing a constant force equal to the force generated by the fluid resistance in the absence of a surface has not been answered definitively. However, experimental studies performed by Lowe et al. (1987) support this hypothesis. The condition of a nearly spherical cell body is approximately satisfied for short, rod-shaped cells, such as *Escherichia coli*, but is poorly satisfied by cells of other body shapes, such as *Spirillum volutans*, which has a thin, spiral-shaped body.

Equation 1b was derived for spherical particles moving perpendicularly toward a solid surface or, as illustrated in Figure 1, approaching the surface at an angle of 0°.

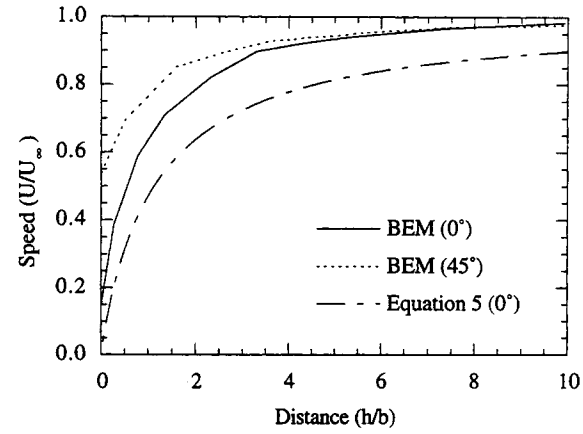

Figure 2. Model solutions.

The speed decrease predicted by Eq. 5 (– – –) for an orientation angle of 0° (perpendicular to and toward the surface) is smaller at a given surface-to-cell separation distance than the boundary element solutions (BEM) of Ramia et al. at the same orientation angle (——). Also, the BEM solution at an orientation angle of 45° (– – –) predicts a higher swimming speed for a given distance than at an orientation angle of 0°.

Other researchers have developed more complex models specifically for describing microbial motion through fluids and near surfaces in an effort to allow for arbitrary cell-body shapes, orientations, and body appendages. For example, the model of Ramia et al. (1993) is based on a cell with a body that can be of arbitrary shape and with a single helical flagellum behind the body, rotating at a constant speed, producing the thrust that propels the cell through the fluid. The authors solved the fluid-dynamics problem posed by the physical model with the boundary-element method (BEM), a numerical technique. Both the models of Brenner and Ramia et al. predict that a spherical cell moving toward a solid surface would experience an increase in drag and therefore, if the cell is unable to compensate by increasing its thrust, also a decrease in its swimming speed. Figure 2 shows the dependence of the bacterial swimming speed on the separation distance for Eq. 5 and for the BEM solutions of Ramia et al. At 10 μm ($h/b = 10$) from the solid surface, the analytical solution given in Eq. 5 predicts that the swimming speed of a bacterium moving perpendicularly toward a solid surface is approximately 90% of its value in the fluid far from solid surfaces, while the BEM solution predicts the speed will be nearly equal to its value in the bulk fluid at this separation distance.

We outline the experimental methods used to collect and analyze the data for the swimming speeds of bacteria moving near a planar glass surface and compare the results to the theoretical solutions discussed earlier.

Methods

In this study, we used a tracking microscope capable of following the three-dimensional motion of individual bacterial cells (Berg, 1971, 1978). A sample containing a dilute suspension of bacteria was placed in a small, cylindrical metal chamber with glass windows on the top and bottom of the

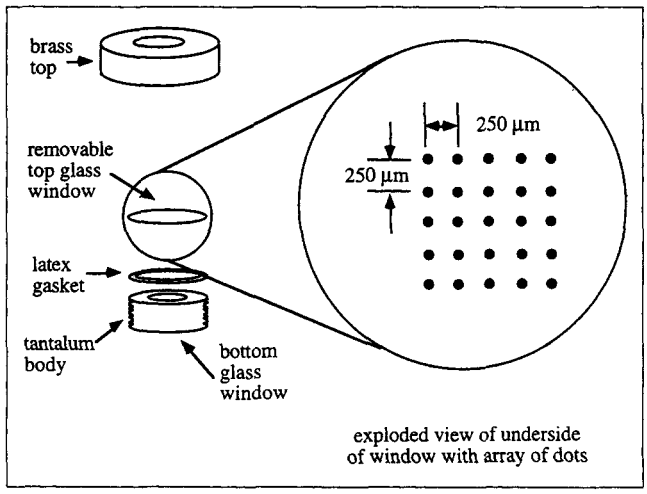

Figure 3. Tracking chamber.

The outer dimensions of the cylindrical lower chamber body were approximately 3.2 mm in diameter by 1.3-mm in height. The lower glass window was sealed with silicone adhesive. The removable upper window was imprinted with an array of chromium dots to allow the location of the surface of the glass.

chamber. The top window of the chamber was imprinted with an array of chromium dots for the purpose of locating the surface of the glass (see Figure 3). The raw data of the experiment, consisting of the x, y and z coordinates of the tracked cell recorded every 1/12 s, was digitized with a 16-bit A/D converter (National Instruments NB-MIO-16XH) and stored on a desktop computer. The data were later analyzed off-line, as in Berg and Brown (1972), to distinguish intervals during which the cell swam smoothly (called runs) from those in which it changed direction rapidly with little net displacement (called tumbles).

The bacterial cells used in the tracking experiments were wild-type (bacteria with a naturally occurring genotype) *Escherichia coli* strain NR50 (from the culture collection of the University of Pennsylvania). Frozen 100-μm aliquots of stock culture were prepared by growing a sample of genetically identical cells from a single colony-forming unit on an agar plate. The cells used in the experiment were grown to midexponential phase by thawing and injecting the frozen 100-μL aliquots of stock culture in 125-mL shaker flasks containing a minimal salts medium at 30°C. The inorganic portion was that used by Adler and Dahl (1967); it was supplemented with galactose (100 g/L) and thiamine (0.5 g/L). The cells were harvested by filtering 10 mL of the culture with five successive rinses of a phosphate buffer solution (0.1-M potassium phosphate, pH 7.0, 10^{-4} M EDTA) using the procedure of Berg and Turner (1990). After filtering, the cells were resuspended in the buffer solution amended with 0.18% w/v hydroxypropyl methylcellulose (Methocel 90 HG, Fluka). The addition of methylcellulose decreases the tendency of cells to wobble while swimming (Berg and Brown, 1972), making it easier for the data-analysis algorithm to discriminate between runs and tumbles. An aliquot of the final suspension (about 10^7 cells/mL) was placed in the tracking chamber and the top window was sealed in place against a latex gasket with a threaded brass top.

The position of the glass surface in contact with the sample was determined by focusing the microscope on the chromium dots (see Figure 3) and recording the stage position. During an experiment, the position of the surface indicated by this calibration drifted slowly in a systematic fashion. This was evident from cell traces in which both the bacterium and the surface were in clear focus (within 1–2 μm of the surface), while the original calibration indicated separations as large as 8 μm at the end of a typical experiment [see Frymier et al. (1995)]. For traces of such bacteria, the systematic error associated with calibrating the position of the surface for cells can be removed by subtracting the distance corresponding to the closest approach of the cell to the surface from all of the experimentally recorded surface-to-cell distances for that cell. This was done in the data shown in Figure 7 to more accurately represent the actual distance between the cell and the surface. However, most of the cells observed did not spend a significant amount of time swimming along the surface, so the systematic error associated with the drift in the surface calibration was not accounted for in the statistical data presented here. The result is that, while the predicted velocities are unaffected, the measured distances from the glass surface to the individual cells can be overestimated by up to 8 μm for the last bacteria tracked, depending on the duration of the experiment; however, most of the data are collected for relatively short experiments and we have determined that the average error in the distance measurements between the beginning and end of a typical experiment is about 4 μm.

Results and Discussion

Figure 4 is a computer reconstruction of the tracking data collected for a typical wild-type bacterium swimming far from

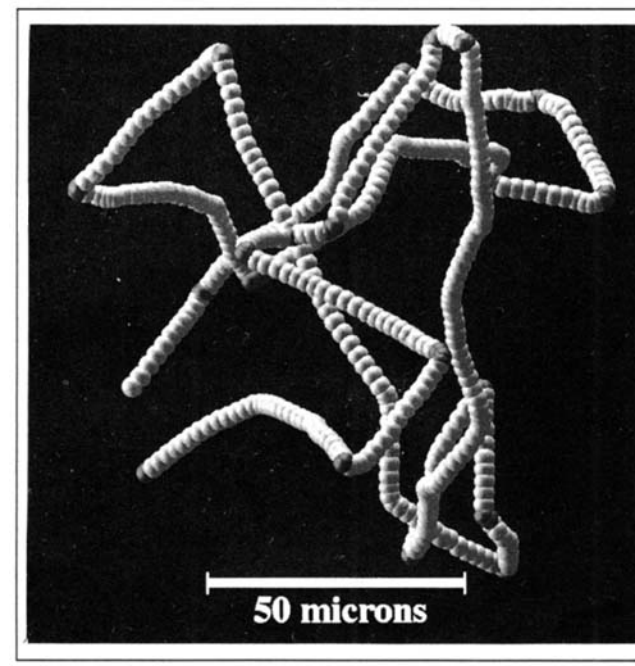

Figure 4. Bacterial motion far from surfaces.

The trace shown is a computer reconstruction of the tracking data from one bacterium moving far (> 400 μm) from solid surfaces. Tumbles are indicated by darker-shaded spheres and runs by a series of lighter-shaded spheres.

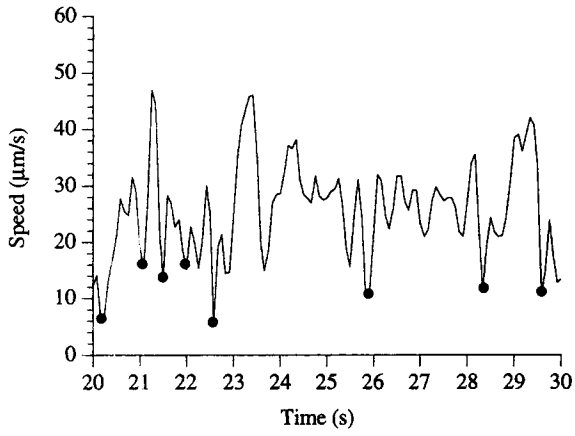

Figure 5. Swimming speed far from surfaces.

The solid dots (●) along the speed trace indicate points at which the bacterium was observed to tumble. Swimming speed drops significantly near a tumble (see data near 20 s, 21 s. 21.5 s, 22 s, etc.). It also varies significantly during a single run (see the run between 22.5 s and 26 s).

a solid surface. This figure illustrates the typical swimming pattern of motile wild-type bacteria, motion in nearly straight paths punctuated by nearly instantaneous changes in direction. Tumbles are indicated by darker shaded spheres and runs by a series of lighter shaded spheres. The spheres were drawn at the x, y, and z coordinates of the bacterium as recorded every 1/12 s.

As a wild-type bacterium swims through a fluid, its speed varies significantly. When a bacterium tumbles, its speed is reduced temporarily as it changes direction. In addition, a cell's swimming speed will vary somewhat even during a single run. Figure 5 is the speed of the bacterium of Figure 4 between the 20th and 30th second of the tracking experiment. The solid dots along the speed data indicate points at which the bacterium executed a tumble. The speed fluctuation near a tumble is evident in this figure near 20 s, 21 s, 21.5 s, 22 s, and so on. Also, the variation in this cell's swimming speed independent of changes due to tumbling can be seen. For example, the speed for the run between 22.5 s and 26 s varies between a high of 43 μm/s at 23.5 s and a low of approximately 14.5 μm/s also occurring near 23.5 s and again near 25.5 s.

The trace of a bacterium tracked near the glass surface is shown in Figure 6. The speed, surface-to-cell distance, and orientation of the cell as a function of the tracking time are shown in Figure 7. The solid black dots on the distance curve indicate points at which the bacterium tumbled. Nearly perpendicular approaches to the surface are indicated in the right portion of Figure 7 by orientation angles close to 0°. There are several points along the trace at which the cell came very near the solid surface (near 1.5 s, 6 s, and 13 s in the left portion of Figure 7) after swimming at some distance from the surface. These points roughly correlate with decreases in the cell swimming speed. However, we are not able to draw definite conclusions about the effect of the surface on the cell swimming speed from this single trace. In a previous study, we analyzed traces from several individual cells to illustrate in an antecdotal fashion the decrease in swimming speed associated with motion directed toward the surface (Frymier et al., 1995). Our purpose in this work is to illustrate that this correlation holds when a large population of cells is studied, instead of a few select traces.

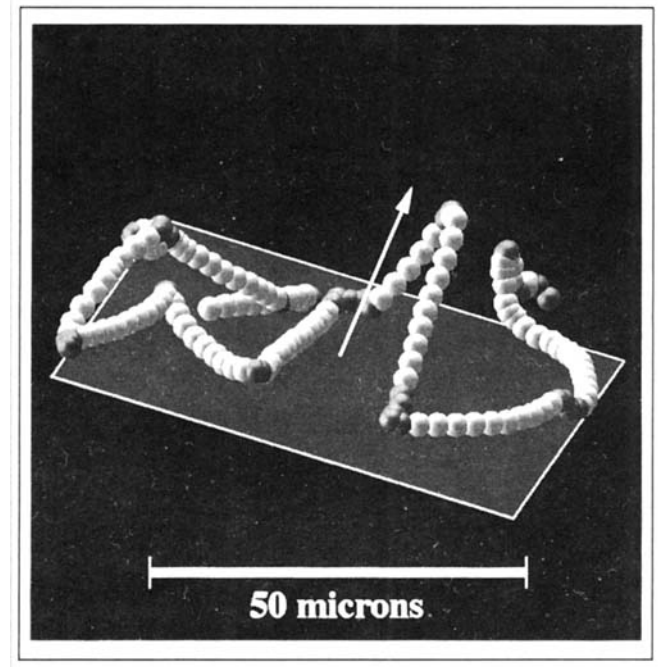

Figure 6. Bacterial motion near a surface.

The location of the solid glass surface is indicated by the flat gray plane. The normal to the plane is indicated by the white arrow. As in Figure 4, tumbles are indicated by darker-shaded spheres and runs by a series of lighter-shaded spheres.

The solution of Ramia et al. (1993) (Figure 2) predicts a finite speed for $h = 0$ (that is, cells collide with the surface). It is difficult to distinguish visually when a cell collides with the surface unless the glass slide has slight imperfections on the surface that come into focus suddenly as the cell approaches the surface. The most useful evidence of whether or not cells collide with the surface is Figure 7 in which the separation distance (indications by the dashed line) decreases suddenly from 10 μm at 1 s to less than 1 μm at around 1.8 s. To the accuracy of the equipment, this indicates contact be-

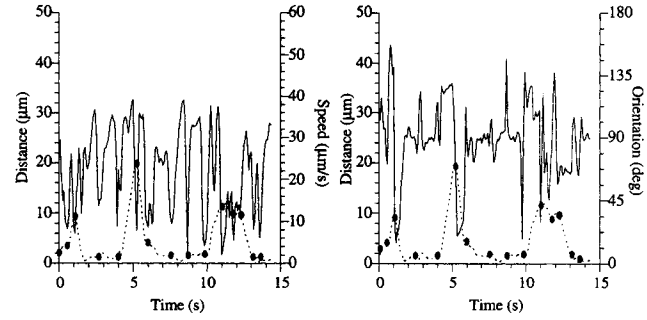

Figure 7. Speed, distance, and orientation near a surface.

On the left, the swimming speed (——) and surface-to-cell distance (– – –) are plotted as functions of the tracking time. On the right, the surface-to-cell distance (– – –) and the orientation to the surface (——) are plotted as functions of the tracking time. The solid dots (●) indicate the occurrence of tumbles.

tween the cell and the surface. This result confirms the result of Ramia et al. that cells have a finite nonzero swimming speed when they collide with a solid surface.

In order to obtain a useful measure of the change in bacterial swimming speeds for wild-type cells near solid surfaces, we used the tracking microscope to study the motion of a total of 90 cells and calculated the average swimming speeds of individual bacteria as a function of the orientation of the cell (whether the cell was swimming toward, approximately parallel to, or away from the surface) and the distance between the cell and the solid surface. At each sample point the speed, cell orientation, and distance between the cell and the glass surface were determined off-line by the data-analysis algorithm.

Four ranges of cell orientation angles (see Figure 1) were used to form the distribution of cell speeds: 0°–45°, 45°–90°, 90°–135°, and 135°–180°. Two ranges of surface-to-cell distances were used: <10 μm and >10 μm. We determined that these distance ranges were appropriate based on the models of Ramia et al. (1993) and Brenner (1961) given previously. Assuming a spherically shaped cell with a radius of 1 μm, when the center of the cell is 10 μm from the surface, Brenner's analytical solution (Eq. 1b) predicts that the drag on a sphere moving perpendicularly toward a solid surface will be approximately 10% greater than its value in the absence of a surface.

We calculated the mean speed during runs for each bacterium that occupied each of the possible eight regions of the distribution (four possible orientation and two distance ranges). For example, a bacterium's trace was analyzed to determine the number of sample points and the swimming speed at each of these sample points for each of the eight distance-orientation ranges (<10 μm at 0°–45°, >10 μm at 0°–45°, ..., <10 μm at 135°–180°, >10 μm at 135°–180°). The mean swimming speed in each range for which samples existed (not all bacteria had data from each of the eight regions) was calculated by dividing the sum of the swimming speeds at each sample point in a particular distance-orientation range by the number of samples in the range. The mean swimming speed for each bacterium in each region calculated in this way was used to form the population statistics so that each bacterium was represented once in each range it occupied.

The mean swimming speed for bacteria >10 μm from the surface, μ_1, and the mean swimming speed for bacteria <10 μm from the surface, μ_2, were used to determine the difference in the mean swimming speeds, $(\langle X_1\rangle - \langle X_2\rangle)$ for each of the four orientation ranges. The resulting statistics are shown in Figure 8. The length of the bars indicate the $100(1-\alpha)$% confidence interval for $\alpha = 0.05$ on $(\mu_1 - \mu_2)$, where μ_1 and μ_2 are the mean swimming speeds of the populations of cells at >10 μm and <10 μm from the surface, respectively. The confidence interval was calculated using (Milton and Arnold, 1990):

$$\text{conf. int.} = (\langle X_1\rangle - \langle X_2\rangle) \pm t_{\alpha/2}\sqrt{S_1^2/n_1 + S_2^2/n_2}, \quad (6)$$

where S_1 and S_2 are the variances for the sample at >10 μm and <10 μm from the surface, respectively, n_1 and n_2 are the numbers of samples, and $t_{\alpha/2}$ is the value of the Student t statistic with $\alpha = 0.05$. The quantity $(\mu_1 - \mu_2)$ is positive for cells moving with orientations in the ranges 0°–45° (perpendicular to and toward the surface) and 135°–180° (perpendicular to and away from the surface). This indicates that the swimming speed for cells <10 μm from the surface in these orientation ranges was less than that for cells at >10 μm from the solid surface. However, $(\mu_1 - \mu_2)$ was nearly 0 for the cell orientations most parallel to the surface, 45°–90° and 90°–135°. Therefore cells swimming approximately parallel and close to the surface swam at a speed close to their speed far from surfaces.

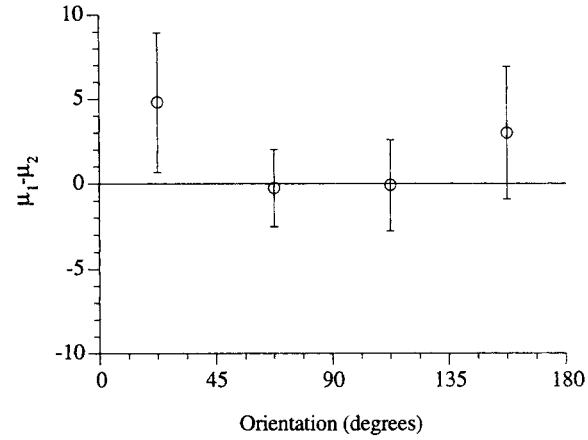

Figure 8. Experimentally observed bacterial swimming speeds.

The difference between the mean swimming speed at distances >10 μm, $\langle X_1\rangle$, and at distances <10 μm, $\langle X_2\rangle$ is plotted as a function of the cell orientation angle. The bars on the data represent the 95% confidence intervals on the value of the population parameter $(\mu_1 - \mu_2)$.

The 95% confidence bars shown in Figure 8 bracket $(\mu_1 - \mu_2) = 0$ for all cell orientations except for cells moving with orientation angles less than 45°, indicating that the difference in mean run speeds is significant for cells moving the most perpendicular to and toward the glass surface. In this range of cell orientations, the difference in mean run speeds for the populations close to and far from the surface is approximately 5 μm/s. This is consistent with the two theoretical predictions shown in Figure 2 that indicate the swimming speed of a cell moving toward a solid surface will decrease as the separation between the cell and the surface decreases. A theoretical value for the mean swimming speed of a cell moving perpendicular to and toward the surface at less than 10 μm may be calculated using:

$$\langle U^*_{<10\ \mu\text{m}}\rangle = \frac{1}{10}\int_0^{10} U^*(h/b)d(h/b), \quad (7)$$

where $U^* = U/U_\infty$. Performing this integration using Eq. 5 for U^* gives $\langle U^*_{<10\ \mu\text{m}}\rangle \cong 0.74$. Using the value for the mean run speed far from the solid surface μ_1 for this sample of 28 μm/s, we have $(\mu_1 - \mu_2)_{\text{theoretical}} \cong (28\ \mu\text{m/s})(1 - 0.74) = 7.3$ μm/s.

This difference is greater than the experimentally observed value of approximately 5 μm/s, although it is within the 95% confidence limits. Performing the integration indicated in Eq. 7 for the BEM solutions of Ramia et al. gives $(\mu_1 -$

$\mu_2)_{\text{theoretical}} = 3.2$ μm/s for an orientation angle of 0°, and $(\mu_1 - \mu_2)_{\text{theoretical}} = 2.4$ μm/s for an orientation angle of 45°. Both of these values are less than the experimentally observed value, but again are within the 95% confidence level.

As discussed previously, the drift in the surface calibration led to experimentally measured surface-to-cell distances that were probably greater for some bacteria (by approximately 4 μm) than the actual distance. Considering this fact, the actual difference between the experimentally observed swimming speed near the surface and that far from the surface was probably less than the measured difference of 5 μm/s. This would decrease the discrepancy between the experimentally observed value of the difference $(\mu_1 - \mu_2)$ and the value predicted using the solutions of Ramia et al. (1993).

While this effect would tend to increase the discrepancy between the experimental value of $(\mu_1 - \mu_2)$ and the value obtained using Eq. 5 in Eq. 7, one must recall that Eq. 5 assumes that the bacterium is moving at an orientation angle of 0°, while the experimental value was obtained using bacteria moving at orientation angles between 0° and 45°. As can be seen in the two BEM solutions in Figure 2, the effect of increasing the orientation angle is to increase the average speed near the surface. This would partially compensate for the increasing discrepancy expected when accounting for the drift in the distance measurement.

Conclusion

Theories based on hydrodynamic considerations have predicted that the speed of a bacterium will decrease as the bacterium approaches a solid surface. In one case (the model of Ramia et al.), a flagellar bundle rotating at a constant rate was assumed, and in the other (based on Brenner's solution of Stokes' equation for a sphere moving in a viscous fluid), a flagellar bundle that produces a constant force. In this study, we found that populations of bacteria within 10 μm of a solid surface and moving toward (with orientation angles between 0° and 45°) the surface had significantly lower mean swimming speeds than those at distances greater than 10 μm. The decrease in swimming speed observed experimentally (5 μm/s) was close to, though slightly higher than that expected based on the model of Ramia et al. (between 2.4 and 3.2 μm/s), while slightly lower than that predicted by the analytical solution (7.3 μm/s) based on Brenner's solution to Stokes' equation for the movement of a sphere toward a solid surface. Therefore, the appropriate model for flagellar propulsion likely lies somewhere between the two models. However, further studies are necessary to discriminate between the two models.

Acknowledgments

The authors thank the IBM Corporation for funding through its Environmental Research Program. They also thank Howard Berg for his assistance with the tracking microscope and Peter Cummings for assistance with the graphics rendering. Any opinions, findings, and conclusions or recommendations expressed in this material are those of the authors and do not necessarily reflect the views of the IBM Corporation.

Literature Cited

Adler, J., and M. M. Dahl, "A Method for Measuring the Motility of Bacteria and for Comparing Random and Non-random Motility," *J. Gen. Microbiol.*, **46**, 161 (1967).

Baba, S. A., S. Inomata, M. Ooya, Y. Mogami, and A. Izumi-Kurotani, "Three-dimensional Recording and Measurement of Swimming Paths of Micro-organisms with Two Synchronized Monochrome Cameras," *Rev. Sci. Instrum.*, **62**, 540 (1991).

Berg, H. C., "How to Track Bacteria," *Rev. Sci. Instrum.*, **42**, 868 (1971).

Berg, H. C., "The Tracking Microscope," *Adv. Opt. Electron Microsc.*, **7**, 1 (1978).

Berg, H. C., *Random Walks in Biology*, Princeton Univ. Press, Princeton, NJ (1993).

Berg, H. C., and R. A. Anderson, "Bacteria Swim by Rotating Their Flagellar Filaments," *Nature*, **245**, 380 (1973).

Berg, H. C., and D. A. Brown, "Chemotaxis in *Escherichia coli* Analysed by Three-dimensional Tracking," *Nature*, **239**, 500 (1972).

Berg, H. C., and L. Turner, "Movement of Microorganisms in Viscous Environments," *Nature*, **278**, 349 (1979).

Berg, H. C., and L. Turner, "Chemotaxis of Bacteria in Glass Capillary Arrays," *Biophys. J.*, **58**, 919 (1990).

Brennen, C., and H. Winet, "Fluid Mechanics of Propulsion by Cilia and Flagella," *Annu. Rev. Fluid Mech.*, **9**, 339 (1977).

Brenner, H., "The Slow Motion of a Sphere through a Viscous Fluid Towards a Plane Surface," *Chem. Eng. Sci.*, **16**, 242 (1961).

Chwang, A. T., T. Y. Wu, and H. Winet, "Locomotion of Spirilla," *Biophys. J.*, **12**, 1549 (1972).

Eliashberg, N., and J. Keasling, "Simulation of Bacterial Growth and Substrate Utilization in a Polluted Groundwater Environment," AIChE Meeting, Chicago, IL (1996).

Frymier, P. D., R. M. Ford, H. C. Berg, and P. T. Cummings, "Three-dimensional Tracking of Motile Bacteria Near a Solid Surface," *Proc. Natl. Acad. Sci. USA*, **92**, 6195 (1995).

Higdon, J. J. L., "A Hydrodynamic Analysis of Flagellar Propulsion," *J. Fluid Mech.*, **90**, 685 (1979a).

Higdon, J. J. L., "A Hydrodynamics of Flagellar Propulsion: Helical Waves," *J. Fluid Mech.*, **94**, 331 (1979b).

Katz, D. F., and J. R. Blake, "On the Movement of Slender Bodies Near Plane Boundaries at Low Reynolds Number," *J. Fluid Mech.*, **72**, 529 (1975).

Lighthill, M. J., "Flagellar Hydrodynamics: the John von Neumann Lecture 1975," *SIAM Rev.*, **18**, 161 (1976).

Lovely, P. S., and F. W. Dalquist, "Statistical Measures of Bacterial Motility and Chemotaxis," *J. Theor. Biol.*, **50**, 477 (1975).

Lowe, G., M. Meister, and H. C. Berg, "Rapid Rotation of Flagellar Bundles in Swimming Bacteria," *Nature*, **325**, 637 (1987).

Lui, Z., and K. Papadopoulos, "Unidirectional Motility of *Escherichia coli* in Restrictive Capillaries," *Appl. Environ. Microbiol.*, **61**, 3567 (1995).

Manson, M. D., P. M. Tedesco, and H. C. Berg, "Energetics of Flagellar Rotation in Bacteria," *J. Mol. Biol.*, **138**, 541 (1980).

Milton, J. S., and J. C. Arnold, *Introduction to Probability and Statistics: Principles and Applications for Engineering and the Computing Sciences*, McGraw-Hill, New York (1990).

Myerscough, M. R., and M. A. Swan, "A Model for Swimming Unipolar Spirilla," *J. Theor. Biol.*, **139**, 201 (1989).

Phan-Thien, N., T. Tran-Cong, and M. Ramia, "A Boundary-element Analysis of Flagellar Propulsion," *J. Fluid Mech.*, **184**, 533 (1987).

Ramia, M., and M. A. Swan, "The Swimming of Unipolar Cells of *Spirillum Volutans*: Theory and Observations," *J. Exp. Biol.*, **187**, 75 (1994).

Ramia, H., D. L. Tullock, and N. Phan-Thien, "The Role of Hydrodynamic Interaction in the Locomotion of Microorganisms," *Biophys. J.*, **65**, 755 (1993).

Reynolds, A. J., "The Swimming of Minute Organisms," *J. Fluid Mech.*, **23**, 241 (1965).

Schneider, W. R., and R. N. Doetsch, "Effect of Viscosity on Bacterial Motility," *J. Bacteriol.*, **117**, 696 (1974).

Stocker, B. A. D., "Bacterial Flagella: Morphology, Constitution, and Inheritance," *Proc. Symp. Society for General Microbiology*, Vol. 6 (1956).

Winet, H., and S. R. Keller, "Spirillum Swimming: Theory and Observations of Propulsion by the Flagellar Bundle," *J. Exp. Biol.*, **65**, 577 (1976).

Manuscript received Nov. 27, 1995, and revision received Dec. 9, 1996.